RAIRO-Oper. Res. 58 (2024) 3501–3519
https://doi.org/10.1051/ro/2024099

RAIRO Operations Research
www.rairo-ro.org

PREDICTION METHOD FOR POWER FLUCTUATIONS IN CROSS REGIONAL CONSUMPTION AND TRANSPORTATION UNDER THE INTEGRATION OF NEW ENERGY

Yajie Li[1,2,3,*], Tao Wang[1,2,3], Shuting Chen[1,2,3], Xinmiao Hu[1,2,3], Rui Yin[1,2,3] and Jun Yan[4]

Abstract. Against the backdrop of the increasing development of the new energy industry, the volatility of new energy output poses significant challenges to regional power grid balance and energy absorption. Therefore, this article proposes a prediction method for cross regional transmission power fluctuations under new energy integration conditions. A comprehensive and representative sample dataset was constructed by comprehensively considering factors such as fluctuations in new energy output, capacity confidence, and peak shaving characteristic parameters, combined with numerical weather forecast data. Normalize the sample data to eliminate dimensional differences between parameters. The sparrow search algorithm is used to optimize the weights and thresholds of the double hidden layer BP neural network, effectively avoiding local optimization problems caused by over training. The experimental results show that this method has significant advantages in predicting power fluctuations in cross regional absorption and transportation of new energy, with a predicted power to power ratio of over 0.85.

Mathematics Subject Classification. 68P99.

Received October 10, 2023. Accepted May 2, 2024.

1. Introduction

With the increasing global demand for renewable energy, new energy sources such as wind and solar energy are gradually becoming the mainstay of the power system. However, the output power of these new energy sources is influenced by natural conditions, such as wind speed and light, and exhibits significant fluctuations [1]. This volatility poses a huge challenge to the stable operation of regional power grids, which may lead to issues such as power grid imbalance and energy waste. In order to fully utilize new energy and ensure the stable operation of the power grid, accurate prediction of the output power of new energy has become crucial.

Keywords. Double hidden layer, BP neural network, new energy, trans regional absorption, transmission power, sine normalization.

[1] State Grid Xinjiang Electric Power Co., Ltd., Information and Communication Company, Urumqi 832000, P.R. China.

[2] State Grid Xinjiang Electric Power Co., Ltd, Urumqi 832000, P.R. China.

[3] Xinjiang Energy Internet Big Data Laboratory, Urumqi, P.R. China.

[4] Nanjing Nari Information and Communication Technology Co., Ltd, Jiangsu, Nanjing 211100, P.R. China.

*Corresponding author: you89624769@163.com

© The authors. Published by EDP Sciences, ROADEF, SMAI 2024

This is an Open Access article distributed under the terms of the Creative Commons Attribution License (https://creativecommons.org/licenses/by/4.0), which permits unrestricted use, distribution, and reproduction in any medium, provided the original work is properly cited.

Gholami *et al.* proposed a power prediction model based on deep learning. The application of this model can improve the trans regional absorption level of new energy to a certain extent, but it does not take into account the impact of the volatility of new energy processing on the prediction results, resulting in low accuracy of the prediction results [2]. However, the impact of fluctuations in new energy processing on the prediction results has not been fully considered, which may lead to limited prediction accuracy. Carrera *et al.* used weather forecast information, latitude, longitude and other geographical information to forecast photovoltaic power generation, studied the factors affecting the output power of photovoltaic power generation, and took into account the impact of various meteorological factors on the cross regional absorption of photovoltaic energy when modeling, but the algorithm relies on detailed meteorological data [3]. But its algorithm highly relies on detailed meteorological data. However, obtaining these detailed data may pose certain difficulties, especially in some remote or poorly monitored areas, which limits the universality and practicality of the model. Memarzadeh G *et al.* studied a new hybrid forecasting model for short-term power load forecasting. Firstly, wavelet transform is used to eliminate the fluctuation behavior of power load and price time series, and feature selection based on entropy and mutual information is used to sort candidate inputs according to their information values and eliminate redundant inputs, and to obtain the accuracy of accurate prediction results through LSTM network in deep learning algorithm. The performance of the proposed method has been successfully verified on load and price data collected by the Pennsylvania–New Jersey–Maryland (PJM) and Spanish electricity markets [4]. But its algorithm is difficult to describe the output characteristics of new energy in real time. This means that these methods may have a certain lag in responding to the rapid changes in new energy output, and cannot provide accurate prediction results in a timely manner. In the existing methods for evaluating the trans regional delivery of new energy, the probability model is established based on stochastic production simulation, which is difficult to describe the output characteristics of new energy in real time; Based on the time-series production simulation method, only the regional new energy absorptive capacity model and analysis method are given, and it is impossible to accurately calculate the trans regional tie line transmission electricity.

As new energy has the characteristics of large fluctuation and large amount of data [5], BP neural network, as a single hidden layer neural network, has the advantages of simple prediction structure and convenient training, and can be used to predict the fluctuation of trans regional absorption and transmission power of new energy. In view of the current application status and shortcomings of BP neural network in the field of new energy trans regional absorption transmission power fluctuation prediction of single hidden layer and batch processing, neural network prediction with multiple hidden layers can often accurately complete a more complex mapping, and the prediction accuracy of double hidden layer BP neural network model is higher than that of single hidden layer network model. Moreover, it can better track the fluctuation of the real value on the trend, and is more suitable for the prediction of new energy absorption and transmission power. Therefore, this paper studies the intelligent prediction method of power fluctuation of new energy trans regional absorption transmission based on double hidden layer BP neural network. The sparrow search algorithm is used to optimize the weights and thresholds of the neural network. This optimization algorithm can search for the optimal solution on a global scale, avoid local optimization problems, and thus improve the prediction accuracy of the model. Taking into account various influencing factors, including the volatility of new energy output, capacity confidence, peak shaving characteristic parameters, and numerical weather forecast data, the model can more comprehensively reflect the actual operation status of new energy. By normalizing preprocessing, the difference dimension of each parameter is eliminated, making the data distribution more uniform, which is beneficial for the training of neural networks and improves the predictive performance of the model.

2. Intelligent prediction of power fluctuation of trans regional absorption and transmission of new energy

The intelligent prediction process of new energy trans regional absorption transmission power fluctuation based on improved double hidden layer BP neural network is shown in Figure 1. The specific steps are as follows:

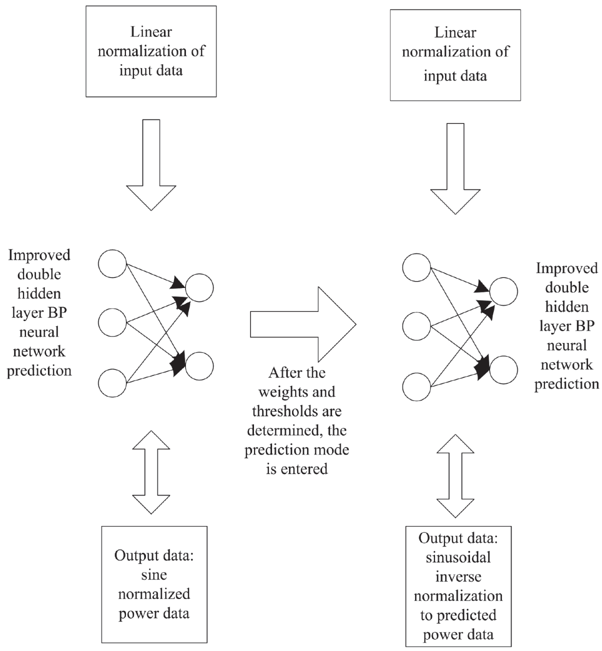

Figure 1. Intelligent prediction process for power fluctuation in new energy cross regional absorption and transportation based on improved double hidden layer BP neural network.

Step 1. Determine the double hidden layer BP neural network structure and initialize the weight and threshold;

Step 2. Conduct linear normalization pretreatment on the sample data input by the double hidden layer BP neural network, and conduct sine normalization pretreatment on the power data obtained by prediction;

Step 3. Set the training mode of the double hidden layer BP network, optimize the threshold and weight of the double hidden layer BP neural network based on the sparrow search algorithm, and improve the prediction effect of the model double hidden layer BP neural network;

Step 4. Linearly normalize the data of the time period to be measured and input the established double hidden layer BP neural network;

Step 5. Sinusoidal inverse normalization is performed on the output data to obtain the intelligent prediction value of new energy trans regional absorption transmission power fluctuation.

2.1. Determination of fluctuation sample data

The absorption capacity of new energy is influenced by various factors, among which the volatility of new energy output, capacity confidence, and peak shaving characteristics are three key factors. Firstly, the volatility of new energy output is one of the important factors affecting the absorption capacity of new energy. Due to various unpredictable factors such as wind speed and light intensity, the output power of new energy is subject to significant fluctuations. This volatility may lead to stability issues in the power grid and affect the absorption capacity of new energy. Secondly, capacity confidence is also an important factor affecting the absorption capacity of new energy. Capacity confidence refers to the maximum power generation capacity that new energy generation equipment can provide within a certain period of time. The higher the confidence level of capacity, the more electricity the new energy generation equipment can provide, which helps to improve the absorption capacity of new energy. Finally, peak shaving characteristics are also one of the factors affecting the absorption capacity of new energy. Peak shaving refers to adjusting the power generation of power generation equipment in a timely manner based on changes in the load of the power grid, in order to ensure the stable operation of the power grid. New energy generation equipment also needs to have peak shaving capabilities to meet the needs of the power grid. Therefore, when predicting the absorptive capacity of new energy in a region, it is necessary to comprehensively consider the above factors, build a sample dataset for predicting the trans regional absorptive transmission power of new energy from the aspect of the new energy's own output characteristics, and use it as the input of the double hidden layer BP neural network to realize the trans regional absorptive transmission power prediction of new energy [6].

2.1.1. *Fluctuation characteristics*

The power fluctuation rate is an indicator reflecting the power fluctuation characteristics of new energy, which can reflect the power variation characteristics of new energy in a large time scale. The power fluctuation of new energy generation will seriously affect the peak shaving of the transmission network, thus affecting the ability of the grid to absorb new energy across regions [7]. This paper introduces an index that reflects the power fluctuation characteristics of trans regional absorption and transmission of new energy: power fluctuation rate. The daily power fluctuation rate prediction [8] is shown in formula (1). For the statistical periods of month and year, the probability of a power volatility interval $F_{di} \sim F_{dj}$ is shown in equations (2) and (3):

$$F_d = \frac{P_{d\max} - P_{d\min}}{p_{GN}} \times 100\% \tag{1}$$

$$\text{Monthly fluctuation probability} = \frac{\text{Daily fluctuation probability range } [F_{di}, F_{dj}]}{\text{Natural days within the month}} \times 100\% \tag{2}$$

$$\text{Year fluctuation probability} = \frac{\text{Daily volatility range } [F_{di}, F_{dj}]}{\text{Natural days within the year}} \times 100\% \tag{3}$$

where: F_d is the daily power fluctuation rate; $F_{d\max}$ is the maximum power of the unit in a day; $F_{d\min}$ is the minimum power of the unit in a day; P_{GN} is the rated power of the unit.

The output change rate describes the output change of new energy power plants within a certain time scale, which is not only reflected in the daily output characteristics, but also has a large seasonal change. The first order difference is used to describe the ratio between the output change value in a specific period and its installed capacity, which is the output change rate σ, as shown in formula (4).

$$\sigma = \frac{\Delta p}{p_{GN}} = \frac{P(t+\Delta t) - P(t)}{P_{GN}} \tag{4}$$

where: p_{GN} is the rated output of the unit, t is the unit operation time.

2.1.2. *Capacity confidence*

Under the operating conditions of the power system, the load carrying capacity of wind power and photovoltaic units with the same capacity is different from that of conventional thermal power and hydropower units [9], so the capacity credit (CC) of wind farms and photovoltaic power plants is significantly different from that of traditional power sources. Capacity confidence refers to the proportion of the capacity of new energy that can replace conventional units in the installed capacity of new energy on the premise of equal reliability. Due to the volatility and randomness of new energy, it is generally considered as a power supply that only provides electricity and does not provide capacity value, so it is necessary to evaluate its capacity value. In this paper, effective load carrying capability (ELCC) is used as the evaluation index of new energy output credibility. This definition ensures that the system maintains the same reliability level before and after the new energy is connected. The calculation of the proportion of the additional load of new energy supply in the installed capacity of grid connected new energy is the new energy power generation capacity confidence. Loss of load expectation (LOLE) is used as an indicator to assess system risk. The mathematical expression of ELCC is:

$$F(C, L) = F(C + \Delta C, L + \Delta L) \tag{5}$$

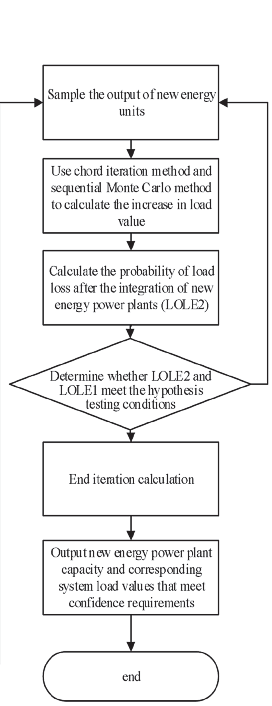

FIGURE 2. Flow chart of capacity confidence algorithm.

$$\text{ELCC} = \frac{\Delta L}{C_{PVN}} * 100\% \tag{6}$$

where: F is expressed as a function of installed capacity and load and system risk indicators; C is the original installed capacity of the system; ΔC is the new energy capacity; L is the original load of the system; ΔL refers to the additional load satisfied by the new power supply, which is the confidence capacity of new energy, C_{PVN} refers to the installed capacity of new energy after grid connection, and the capacity confidence of new energy can be obtained from formula (6) [10].

In this paper, the sequential Monte Carlo method is used to calculate the risk of the power plant without new energy, and LOLE1 is obtained. Then, the risk of the power plant with new energy is calculated, and LOLE2 is obtained. LOLE2 is smaller than LOLE1. The load of the system is increased through iterative calculation until the calculated LOLE2 and LOLE1 meet the hypothesis test conditions. The program flow chart is shown in Figure 2. The basic steps of using sequential Monte Carlo method to calculate the capacity confidence of grid connected new energy power plants are as follows:

(1) The conventional unit adopts a dual state model, namely normal operation and fault state, which is described by normal operation time and maintenance time. The system generator state is sampled to form the generator state sequence, and then the generator capacity sequence is generated;
(2) The risk of power shortage, namely, the probability of load loss, is accumulated by sequential Monte Carlo algorithm;
(3) The output of new energy units is sampled to form the output sequence of new energy, and the load added value is calculated by chord section iteration and sequential Monte Carlo method;
(4) Determine whether LOLE2 after load increase and LOLE1 before new energy increase meet the hypothesis test.

2.1.3. Peak shaving characteristics

The new energy output is superimposed on the original load in a negative form to obtain the new load curve, and the original load peak valley difference and the new load curve load peak valley difference are compared and analyzed. When the original load peak valley difference is large, the new energy output shows positive peak shaving, and when the original load peak valley difference is small, the new energy output shows reverse peak shaving. The calculation formula is as follows:

$$\Delta p_j = p_j^{\max} - p_j^{\min} \tag{7}$$

$$\Delta p_j^n = p_j^{n\max} - p_j^{n\min} \tag{8}$$

$$C_j = \Delta P_J - P_j^{n\min} \tag{9}$$

$$C_j = \frac{C_j}{\Delta P_j} \times 100\% \tag{10}$$

where: $p_j^{\max}$ and $p_j^{\min}$ represent the maximum and minimum values of the system's original load on day j, $p_j^{n\max}$ and $p_j^{n\min}$ represent the maximum and minimum value of new load after the system superimposes new energy on day j, Δp_j and Δp_j^n respectively represent the j-th day peak valley difference of daily original load and new load, C_j represent the change value of the peak and valley difference of the system before and after the new energy access on day j, when $C_j < 0$, it express as anti-peak, C_j is expressed as the contribution rate of new energy daily peak shaving.

2.2. Input sample data preprocessing method

When the double hidden layer BP neural network is used to predict the trans-regional absorption and transmission power of new energy, the sample data has seven input parameters, each of which has different dimensions. In order to use the parameters with different dimensions equally, it must be normalized, including linear normalization and nonlinear normalization.

2.2.1. Linear normalization method

The normalization problem is put forward. For linear problems, the condition number of the sample data measurement matrix for new energy trans-regional consumption transmission power prediction is an important reason that affects the stability of the algorithm. Assume that the sample data measurement matrix is A, its condition number is defined as: $cond(A) = \left\|A^{-1}\right\|\|A\|$, the condition number can be measured by the singular value of matrix A through the sample data. The condition number is an important index value of the ill-conditioned degree of the equation. The larger the condition number, the more ill-conditioned the equation is, and the less robust the method is. One of the effective ways to improve robustness is to reduce the condition number of sample data measurement matrix. In the process of processing, the observation matrix of sample data may be close to singularity, which leads to a large number of conditions. At this time, if the equation is solved by column principal element elimination method, it may produce zero principal element or very small principal element, which leads to the equation being unsolvable or the result of solving is very wrong. In order to solve this problem, singular value decomposition of matrix can be used to solve it.

Find orthogonal matrix U and V, make $A = UWV^T$, in which: $W = diag(w_1, w_2, \cdots, w_n)$, in w_1, w is the non-negative square root of the n eigenvalues of the matrix A^TA, then the least squares solution of the equation $AH = b$ is attainable. After obtaining the coordinates of other observation data, the transformation matrix can be used to unify them A in the coordinate system, the normalization of observation data of different samples is completed.

If that observation straight line of the sample data are $k(Z_1, Z_2, \cdots, Z_k)$, for straight lines $Z_i = (a_i, b_i, c_i)^T$, make $n_1 = \sum_{i=q}^k a_i n_2 = \sum_{i=1}^k b_i$, $n_3 = \sum_{i=1}^k c_i$, construct the transformation matrix. $N_1 = \begin{pmatrix} 10 - n_1/n_3 \\ 01 - n_2/n_3 \\ 001 \end{pmatrix}$,

$Z_i^1 = \left(a_i^1, b_i^1, c_i^1\right)^T$ after $Z_i^1 = N_1 Z_i$ transformation satisfies $\sum_{i=1}^k a_i^1 = 0$, $\sum_{i=1}^k b_i^1 = 0$, that is, the transformed center of gravity falls on the z-axis, and the z-axis of the transformed linear coordinates is more evenly distributed.

$$s = \left(\frac{\sum_{i=1}^k \left(a_i^1\right)^2 + \left(b_i^1\right)^2}{2\sum_{i=1}^n c_i^2}\right)^{\frac{1}{2}}. \tag{11}$$

Construct transformation matrix N_2 as $N_2 = \begin{pmatrix} 100 \\ 010 \\ 00s \end{pmatrix}$, after $Z_i^2 = N_2 Z_I^1$ transformation, the linear coordinates $Z_i^2 = (a_i^2, b_i^2, c_i^2)$ satisfies: $\sum_{i=1}^k ((a_i^2)^2 + (b_i^2)^2) = 2\sum_{i=1}^k \left(c_i^2\right)^2$. That is, the spatial distribution of the transformed linear coordinates is more uniform.

The main steps of the normalization algorithm are as follows (assuming that the corresponding straight line is $Z_i \leftrightarrow \tilde{Z}_i$);

Step 1. For straight lines Z_i, according to the needs of the above transformation N_1, N_2 and get $Z_i^2 = N_2 N_1 Z_i$;
Step 2. For straight lines $\tilde{Z}_i$, also constructed according to the needs of the above transformation N_1, N_2 and get $Z_i^2 = N_2 N_1 Z_i$;
Step 3. Solve the corresponding straight line by direct linear method $Z_i^2 \leftrightarrow \tilde{Z}_i^2$, the corresponding homography matrix is $\tilde{H}$;
Step 4. Do the inverse transformation of the normalization transformation, get the homography matrix of corresponding straight line $Z_i \leftrightarrow \tilde{Z}_i$.

Through this normalization, it will be more effective to estimate homography matrix by direct linear method. Because the actual power data is not uniform, it is unreasonable to normalize the output value (that is, the power value), so this paper proposes a nonlinear normalization method to solve this problem.

2.2.2. Nonlinear normalization method

Nonlinear normalization is usually used in scenes with large data analysis, and the values are large or small. The original values are mapped by some mathematical functions, and the commonly used functions include log, exponent, tangent, etc., the curve of nonlinear function needs to be determined according to the specific situation of data distribution.

$$x_{\text{new}} = \sin\left(\frac{\pi}{2}x\right). \tag{12}$$

In formula (12), x, x_{new} respectively represent the linear normalized result and the sinusoidal normalized result.

The above sine function has the following characteristics in mathematics: when $x = 0.56$, its slope is equal to that of linear normalization method, and when the independent variable x value is less than 0.56, its slope is greater than that of the straight line in the linear normalization method, and when the value of the independent variable is greater than 0.56, its slope is less than that of the straight line in the linear normalization method. After this transformation, the sample difference in the small power interval is enlarged and the excessive sample difference in the larger power interval is reduced without changing the data. After normalization, the smaller value interval is not dense and the larger value interval is not sparse, which makes the distribution of samples more uniform. This can not only accurately describe the change of lower power, but also accurately predict the value of higher power.

Comparison of sample distribution before and after normalization. After the training is completed, the prediction results should be denormalized, and the process is as follows:

$$x' = \frac{2}{\pi}\sin^{-1}(x_{\text{out}}). \tag{13}$$

In the formula, x_{out}, x' respectively represent the neural network outputs the prediction result of trans-regional absorption and transmission power fluctuation of new energy and the result of sine denormalization.

Then the linear denormalization is performed:

$$x'_{\text{out}} = x'_{\text{out}.p}(M - N) + N. \tag{14}$$

In formula (14), x'_{out}, $x'_{\text{out}.p}$ respectively represent the final denormalization result and the sine denormalization result; M, N are the maximum value and the minimum value in the training sample. Using non-sinusoidal normalization method does not change the original data, but improves the distribution of teacher signal data during training, making full use of the characteristics of data, thus improving the performance of neural network model.

2.3. Improved double hidden layer BP neural network based on sparrow search algorithm

The input parameters of the power forecasting model are the main factors affecting the power, including conventional data such as wind speed, wind direction, temperature and humidity, air pressure, and the fluctuation, capacity confidence and peak shaving characteristics of the new energy output obtained above. The output parameters are the cross-regional consumption power data of new energy, and the model establishes the mapping between the input parameters and the output parameters. When forecasting, the power output parameter value can be obtained by substituting the input parameter value into the model calculation, that is, the predicted cross-regional absorption power of new energy [11].

The input contains a lot of new energy information, and the conventional data are generally obtained by numerical weather forecast [12]. The numerical weather forecast can give a reasonable input for wind farm power prediction [13] considering the essential law of atmospheric motion. During neural network training, the predicted inputs are four parameters [14] of wind speed, wind direction, temperature, humidity and air pressure provided by numerical weather forecast, and three parameters, namely, fluctuation of new energy output, capacity confidence and peak shaving characteristics, totaling seven parameters, and the output is the cross-regional consumption of new energy power at corresponding time.

The research on the network structure of power prediction shows that with the complexity of mapping, the number of hidden layer units should be increased; At the same time, with the increase of the number of samples, the hidden layer units should also be increased appropriately; In terms of function fitting, neural network with a hidden layer is often not the best scheme. There are many factors affecting the cross-power prediction of new energy, such as the relationship between peak value and current control [15]. In order to achieve better prediction accuracy, a large number of samples are needed for network training.

The above theory can be applied to new energy power prediction neural network prediction [16]. When using single hidden layer BP neural network to predict, more hidden layer nodes should be used in theory, which not only increases the training time, but also tends to over-fit, which reduces the generalization ability of the network. Therefore, BP neural network with multiple hidden layers can be considered to predict the fluctuation of trans-regional consumption and transmission power of new energy. Figure 3 is a power prediction structure of double hidden layer BP neural network, in which the number of nodes in two hidden layers can be adjusted. As shown in Figure 3, the function of the input layer is to import the input values of various parameters used in the prediction into the network, so as to carry out forward calculation and output the prediction results of new energy trans-regional consumption and transmission power.

The double hidden layer BP neural network model can dynamically adjust the weights and thresholds in the neural network through multiple trainings [17], so as to improve the prediction accuracy of the trans-regional consumption and transportation power fluctuation of new energy. However, the optimal weights and thresholds in the neural network model can be directly determined through the sparrow search algorithm [18], which avoids the possibility of over-training caused by randomization of weights and thresholds for multiple trainings in the trans-regional consumption and transportation power fluctuation prediction of new energy, and also reduces the possibility of falling into a local optimal solution. In the actual model training, the double hidden layer BP

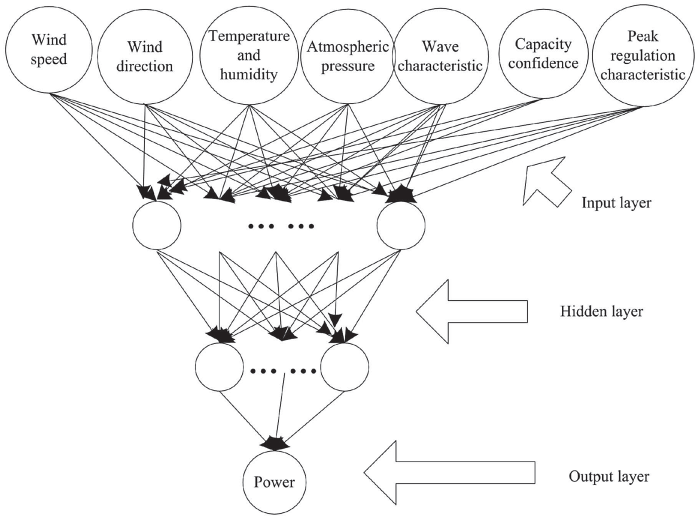

FIGURE 3. Structure diagram of double hidden layer BP neural network model.

neural network has been trained for many times, and the model accuracy is generally too low due to the random initialization of weights and thresholds. Therefore, in order to improve the prediction accuracy of trans-regional consumption and transmission power fluctuation of new energy, this paper aims at the problem that the double hidden layer BP neural network is easy to fall into a minimum due to the random selection of weights and thresholds, and establishes an improved topology structure of double hidden layer BP neural network based on sparrow search algorithm (SSA) [19], that is, SSA-double hidden layer BP neural network. The flow chart of the establishment process is shown in Figure 4.

The process of SSA improving double hidden layer BP neural network is as follows:

(1) Data normalization. Normalize the filtered input and output data, and normalize the data range to $[-1, 1]$. The dimension gap between input data and output data is reduced, which ensures that there will be no convergence speed difference or inability to converge because of the large dimension gap in the training process of the network.

(2) Determine the model structure of double hidden layer BP neural network. Determine the number of nodes in the input layer $v = 7$, the output variable node number $q = 1$, then the empirical formula of the number of double hidden layer nodes p and q is:

$$p = v + q + x. \tag{15}$$

In the formula (15): $x \in [1, 10]$ is any constant. Combined with the experimental data, the root mean square error is used as the criterion, and some data are shown in Table 1.

According to the data in Table 1, the root mean square error of neural network prediction model changes with the number of hidden layers and the number of neurons in hidden layers [20], and it is obtained through many experiments that when $p \in [-5, 5]$, the e value is minimum. Then the final structure of the double-layer BP neural network model based on SSA optimization is 7–5–5–1.

(3) Determine the initialization parameter value. Determine each parameter variable needed in SSA: evolution number maxgen and population size sizepop, where the maximum evolution number is iteration number, and the range of values is generally $[10, 50]$, and the value should not be too large to prevent over-calculation; The range of population size is generally $[20, 100]$. At the same time, the proportion of discoverers is defined as 0.2, and the early warning value and the number of watchmen are set.

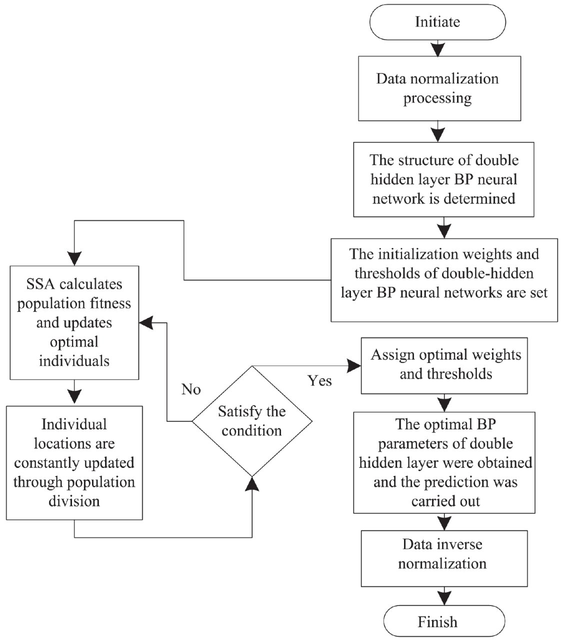

FIGURE 4. SSA improves the flow chart of double hidden layer BP model.

TABLE 1. The relationship between the number of hidden layers and the number of neurons and the root-mean-square error of neural network.

Hidden layer number	4–3	4–4	5–5	5–6	6–6
e	1.201	0.942	0.588	0.756	0.863

(4) SSA calculates population fitness. Through the self-defined adaptive function, the initial weights and thresholds are trained by neural network, and the difference between the predicted value of new energy trans-regional consumption and transportation power and the real value of new energy trans-regional consumption and transportation power is taken as the fitness function value. The smaller the absolute sum of the differences, the smaller the error. Then find the position that produces the minimum value and record it as the global optimal solution. In addition, the dimension size is determined according to the weights and thresholds in the structure of the neural network initially set. Firstly, according to the input node and the first hidden layer node, the first hidden layer node and the second hidden layer node, and the second hidden layer node and the output node, the total number of weights is determined as follows $7\times5+5\times5+5\times1 = 65$; Then, according to the sum of all hidden layer nodes and output layer nodes, the total number of thresholds is determined as $5 + 5 + 1 = 11$, so the dimensions in the topological network structure are $65 + 11 = 76$.

(5) Update that position of sparrows in each part of the population. In the sparrow search algorithm, the location update expression of the discoverer is:

$$X_{i,j}^{t+1} = \begin{cases} X_{i,j}^{t} \exp\left(-\frac{i}{\alpha\, iter_{\max}}\right), & R_2 < \mathrm{ST} \\ X_{i,j}^{t} + QL, & R_2 \geq \mathrm{ST} \end{cases} \tag{16}$$

where: $X_{i,j}^{t+1}$ is the j dimensional position of the i individual in the t generation in the population; α is a random number and takes a value of $(0, 1]$, $iter_{\max}$ represents the maximum number of iterations within a constant; Q is a standard normal distribution random number; L is dimension array of $1 \times d$, d is the dimension; R_2 is the warning value, the value range $[0, 1]$, ST is a safe value, and take the range of value is $[0.5, 1]$.

The follower's position update expression is:

$$X_{i,j}^{t+1} = \begin{cases} Q\exp\left(-\frac{X_{\text{worst}} - X_{i,j}^t}{i^2}\right), & i > \frac{n}{2} \\ X_P^{t+1} + \left|X_{i,j}^t - X_P^{t+1}\right| A^+ L, & i \le \frac{n}{2} \end{cases} \tag{17}$$

where: X_{worst} is the worst position in the whole world; X_P is the optimal position in the iterative process of sparrow population; n is the population size. Formula $A^+ = rand\{-1, 1\} \cdot A^T \left(AA^T\right)^{-1}$. When $i > \frac{n}{2}$, the value is the product of a standard normal distributed random number and an exponential function based on a natural logarithm, when the population converges to match the standard normal distributed random number. When $i \le \frac{n}{2}$, the value is the position of the current optimal sparrow plus the product of the random addition and subtraction of each dimension distance between the sparrow and the optimal position A^+.

In the process of feeding back, some sparrows have the ability of vigilance and investigation, and once they find danger, they will give up food immediately to ensure safety. This part of sparrows accounts for 10%∼20% of the whole population. Assuming that they are randomly distributed in the whole population, the expression of this part of the population is:

$$X_{i,j}^{t+1} = \begin{cases} X_{\text{best}}^t + \beta\left|X_{i,j}^t - X_{\text{best}}^t\right|, & f_i > f_g \\ X_{i,j}^t + K\left[\frac{\left|X_{i,j}^t - X_{\text{worst}}^t\right|}{(f_i - f_w) + \varepsilon}\right], & f_i = f_g \end{cases} \tag{18}$$

where: β is to meet the standard normal distribution of random numbers, the step size of parameters is determined; K is a uniform random number, and the value is $[-1, 1]$, indicating that the direction of sparrow movement is also a step control parameter; ε is a constant, which is used to prevent the denominator from being 0; X_{best} is the best position in the whole world; f_i is the i-th individual fitness value; f_g and f_w are the best and worst fitness values in the current global.

Update the discoverer's position in the group according to formula (16), update the follower's position according to formula (17), and update the vigilante's position randomly distributed in the group accounting for 10%∼20% according to formula (18).

(6) Comparing the fitness after updating the position with the optimal fitness value. Check whether it meets the global optimal solution when the maximum number of iterations is completed. If it meets the global optimal solution, record it, and obtain the best weight and threshold of double hidden layer BP neural network. Otherwise, it will be iterated again.

(7) Assign the values that meet the conditions to the weights and thresholds of the double hidden layer BP neural network to ensure that the topological structure of the double hidden layer BP neural network achieves the optimal accuracy.

(8) The SSA-optimized double hidden layer BP neural network is applied to intelligently predict the fluctuation of trans-regional consumption and transmission power of new energy.

3. Experimental analysis

There are abundant solar and wind energy resources in L area. The research method of this paper takes a new energy distribution network in L area as the research object. The installed capacity of this power station is 1000 MW, and each unit is 2 MW. Each unit is equipped with a new energy power generation component

TABLE 2. Installed capacity of each unit of new energy active distribution network.

Unit type	Installed capacity/MW
Wind turbine 1 installed capacity	961
Wind turbine 2 installed capacity	864
Wind turbine 3 installed capacity	938
Wind turbine 4 installed capacity	907
Pv unit 1 installed capacity	702
Pv unit 2 installed capacity	651
Pv unit 3 installed capacity	683
Pv unit 4 installed capacity	637

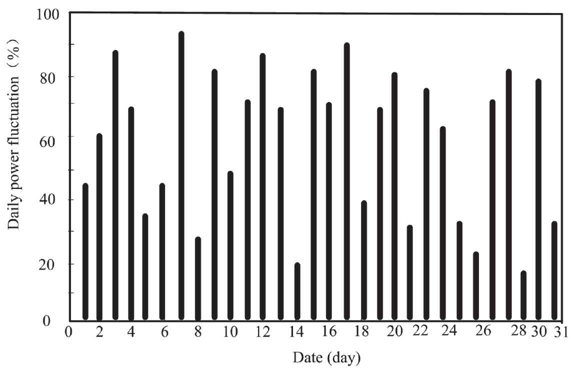

FIGURE 5. Daily power fluctuation.

bracket. This power station is located in the northwest of the city, 30 km away from the city center. According to the data of local weather station, the location of new energy power station is rich in light energy and wind energy resources, which has development value. Taking meteorological conditions as independent variables, the power generation of new energy power stations is predicted. By analyzing the historical data of this power station, it is found that the composition of historical power and influencing factors of the power station is complex and shows strong seasonal characteristics. Therefore, in this experiment, two data in December 2020 and August 2021 are selected as data samples to construct the experimental data set. This data set contains two kinds of data samples, one is a time series with a collection period of 15 min, which can help the subsequent data decomposition and prediction. The installed capacity of each new energy unit in the new energy distribution network is shown in Table 2.

Based on the data of the research object mentioned above, an operational model of the new energy distribution network was constructed on the MATLAB simulation platform to simulate the daily operation of the distribution network. The research model in this paper was input into the simulation model to verify the power prediction performance of the research method.

3.1. New energy trans-regional consumption and transmission power fluctuation analysis

Taking the output data of a wind farm in this new energy distribution network as an example, the daily power fluctuation rate of this wind farm within one month is calculated as shown in Figure 5.

According to Figure 5, the output of wind power is more difficult to predict than that of photovoltaic power, and the daytime active power fluctuation of wind farms is quite different, and the number of days with power fluctuation above 50% in this month is 17 days. From the output change rate of photovoltaic and wind power,

Table 3. Wind power, photovoltaic 15 min output fluctuation characteristics.

Wind power (Daily power fluctuation)				Solar power (15 min output change rate)			
Summertime		Wintertime		Summertime		Wintertime	
Volatility	Chance (%)	Volatility	Chance (%)	Volatility	Chance (%)	Volatility	Chance (%)
0∼20%	7.82*	0–20%	7.01*	−0.1∼0.6	0.07*	−0.1∼0.6	0.02*
20∼40%	16.12	20–40%	19.16*	−0.6∼−0.2	2.65*	−0.6∼−0.2	2.99*
40∼60%	26.92*	40–60%	18.63	−0.2∼0.2	95.11*	−0.2∼0.2	94.1*
60∼80%	20.09*	60–80%	34.98*	0.2∼0.6	2.89	0.2∼0.6	3.51*
80∼100%	31.12*	80–100%	21.09	0.6∼1.0	0.09*	0.6∼1.0	0.03*

Notes. $^{(*)}$Indicates $p < 0.05$.

we can know that wind power fluctuates greatly, so it is impossible to accurately judge the output power in a long period of time; The output change rate of photovoltaic power station is much smaller than that of wind power, and the output power is relatively gentle, which has obvious increase and decrease in a day, reflecting the regularity of photovoltaic power generation being alternated by solar radiation day and night.

Through the distribution of photovoltaic 15 min output and typical daily wind power fluctuation rate of the new energy active distribution network in 2020, the output characteristics of new energy are obtained, which further reflects the difference between wind power output and photovoltaic output. The specific parameter distribution is shown in Table 3. Considering that the distribution of data such as fluctuations in new energy production, capacity confidence, and peak shaving characteristics may not conform to assumptions of normal distribution or homogeneity of variance, non parametric hypothesis testing is used for statistical analysis. To test whether there is a significant difference in production fluctuations between wind and photovoltaic power in different seasons, Wilcoxon signed rank test was used. The null hypothesis for hypothesis testing is that there is no significant difference in the production fluctuations of wind and photovoltaic power in different seasons. If the p-value of the test statistic is less than the significance level (0.05), the null hypothesis is rejected, and it is assumed that there is a significant difference in the production fluctuations of wind and photovoltaic power in different seasons. As can be seen from Table 3, the probability that the output fluctuation of wind power is above 50% in both winter and summer is about 50%, and the output fluctuates greatly. Photovoltaic output is obviously characterized by "small at two ends and large in the middle", which is symmetrical and regular. According to the experimental results, there are significant differences in the yield fluctuations of wind power and photovoltaic in different seasons.

The sequential Monte Carlo method is used to calculate the capacity confidence of typical photovoltaic power plants and wind power plants connected to the new energy active distribution network, and the calculation results are shown in Table 4. Perform Kruskal Wallis test on the production fluctuations of different wind and photovoltaic power plants to examine whether there are significant differences in production fluctuations between them. The null hypothesis for hypothesis testing is that there is no significant difference in output fluctuations among different wind and photovoltaic power plants. If the p-value of the test statistic is less than the significance level (0.05), the null hypothesis is rejected and it is assumed that there are significant differences in output fluctuations among different wind and photovoltaic power plants.

From Table 4, it can be seen that the confidence of new energy capacity in this method is all below 50%, and the confidence of new energy trans-regional consumption and transmission power capacity is low, so it is difficult to connect to the grid on a large scale. According to the experiment, there are significant differences in output fluctuations among different wind and photovoltaic power plants.

The peak-shaving contribution rate of a new energy distribution network in a natural month in L area is shown in Figure 6.

TABLE 4. Capacity confidence of wind power and photovoltaic in new energy active distribution network.

Unit type	Summer capacity confidence/%	Winter capacity confidence/%
Wind turbine 1	25.3*	40.6
Wind turbine 2	26.2*	29.5*
Wind turbine 3	24.8*	29.1*
Wind turbine 4	18.5	34.8
Photovoltaic unit 1	37.88*	30.9*
Photovoltaic unit 2	31.29*	27.3
Photovoltaic unit 3	39.35*	24.9*
Photovoltaic unit 4	24.85*	24.1

Notes. (*)Indicates $p < 0.05$.

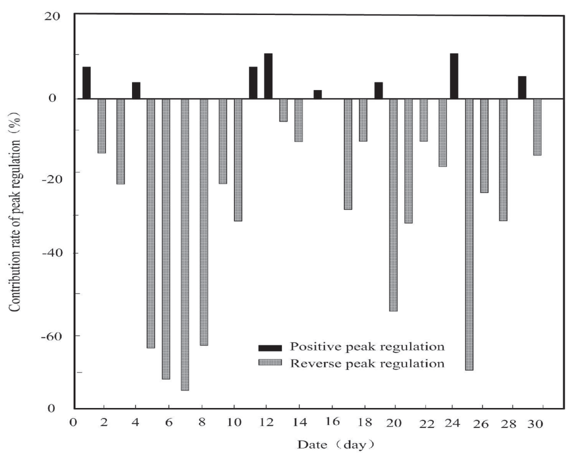

FIGURE 6. Contribution rate of peak regulation.

It can be seen from Figure 6 that there are 20 times of peak reversal, and the peak reversal characteristics are obvious. Therefore, it can be concluded that wind power has obvious anti-peak regulation characteristics. When the grid load is low, wind power does not absorb the system power, on the contrary, it also grabs the power generation; However, at peak hours, its adjustable output is reduced, which increases the output capacity of other generator sets and seriously restricts the consumption of new energy.

Based on the above data, it can be seen that the output of new energy distribution network in this area has significant fluctuation. Therefore, this paper takes the fluctuation of new energy output, capacity confidence and peak shaving characteristics as influencing factors, and combines the conventional data provided by weather forecast, such as wind speed, wind direction, temperature and humidity, air pressure, etc., to construct a sample data set and make an intelligent prediction of the fluctuation of new energy trans-regional consumption and transmission power.

3.2. Data normalization pretreatment effect analysis

Taking the data distribution of power value of wind farm in new energy distribution network as an example, the statistical distribution histogram results are shown in Figure 7.

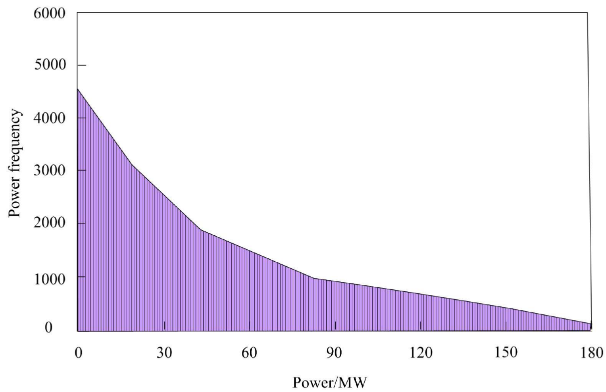

Figure 7. Wind farm power data distribution throughout the year.

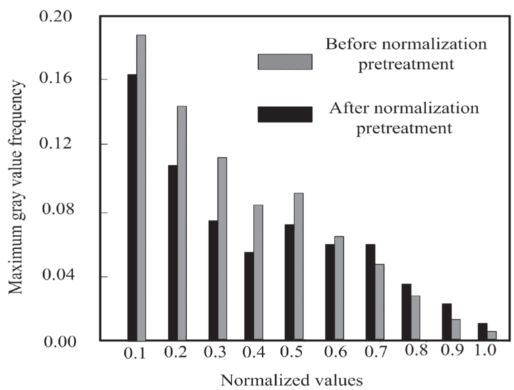

Figure 8. Comparison of effects before and after normalized treatment.

As can be seen from Figure 7, the interval with lower power (*e.g.* 0∼10 MW interval) the number of power samples (11 000) is obviously higher than that in higher power interval (*e.g.* 130∼140 MW) the number of power samples (2500), so the samples in the lower power interval need to be accurately predicted, otherwise the errors will accumulate in a large amount (due to a large number). In addition, it is assumed that the power samples are evenly distributed in the power interval, and in the lower power interval (*e.g.* 0∼10 MW), and the interval between samples is 0.9 kW. This difference will become smaller after linear normalization, and the difference between samples is not obvious, which may cause confusion among the outputs of different inputs in this interval, resulting in errors, which means that the power values used in the establishment of BP neural network power prediction model will be unevenly distributed, which will reduce the accuracy of lower power interval prediction. Correspondingly, in the higher power interval, there is a big difference between samples, but it is easy to produce overtraining. Therefore, evenly distributed samples will be beneficial to the training of neural networks.

Aiming at the above problems, this paper proposes a data normalization preprocessing method. In order to verify the effectiveness of the intelligent prediction method of new energy trans-regional consumption and transportation power fluctuation in this paper, the maximum gray value frequency of the data before and after normalization is compared, and the comparison effect is shown in Figure 8.

As can be seen from Figure 8, the frequency of the maximum gray value of the data after normalization pretreatment is lower than that before normalization pretreatment. The comparison results show that the application of normalization pretreatment method can predict the trend of lower power value more accurately,

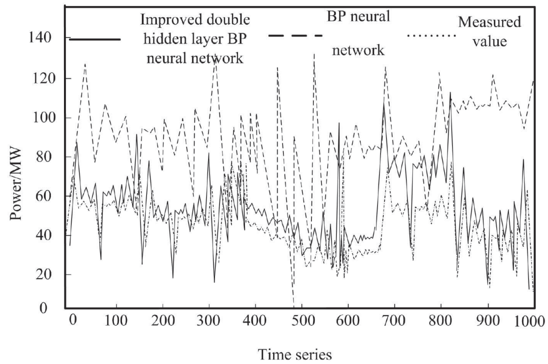

FIGURE 9. The results of improved double-hidden layer BP neural network and BP neural network prediction method are compared.

and the prediction of higher power value is not lost, and the operation is simple, which is more conducive to accurately predicting the absorbed transmission power value.

3.3. Analysis of the effect of intelligent prediction of trans-regional consumption and transmission power of new energy

In order to verify the prediction accuracy of this method using double hidden layer BP neural network, the prediction accuracy of improved double hidden layer BP and single hidden layer BP neural network is compared. Taking 30 541 groups of data of the new energy distribution network in 2020 as training samples and 1000 groups of data in 2021 as test samples, the power prediction models of BP neural network are established with single hidden layer and improved double hidden layer respectively. Figure 7 shows the comparison between the predicted results of the two models and the real results. The vertical axis is power, and the horizontal axis is continuous time series with an interval of 15 min. Table 6 shows the detailed parameters of the prediction results of the two models.

According to the Functional Specification for Wind Power Forecasting System, the calculation formulas of each parameter in Table 6 are shown in formulas (19) and (20).

Mean absolute error (MAE):

$$\mathrm{MAE} = \frac{1}{n}\sum_{n}^{i=1}\left(\frac{|P_{mi} - P_{pi}|}{C_i}\right). \tag{19}$$

In the formula, in P_{mi}, i is the actual average power of the time period; in P_{pi}, i is the predicted power of the time period; in C_i, i is the total boot capacity of the time period; n is the number of all samples.

Correlation coefficient (r)

$$r = \frac{\sum_{i=1}^{n}\left[(P_{mi} - \overline{p_m})(p_{pi} - \overline{p_p})\right]}{\sqrt{\sum_{i=1}^{n}\left(P_{mi} - \overline{p_m}\right)^2 \sum_{i=1}^{n}\left(p_{pi} - \overline{p_p}\right)^2}}. \tag{20}$$

$\overline{p_m}$ represents the average measured power of all samples; $\overline{p_p}$ represents that average value of all predicted pow samples.

According to Figure 9 and Table 5, it can be concluded that the improved double hidden layer BP network has smaller prediction MAE and higher prediction correlation coefficient than the single hidden layer network. The reason is that the power output value of new energy distribution network has the characteristics of large fluctuation and large amount of data, and the double hidden layer network structure is more suitable for its power prediction. The experimental results show that the improved double hidden layer BP neural network model has higher prediction accuracy than the single hidden layer network model.

TABLE 5. Improved prediction accuracy comparison between double hidden layer and single hidden layer BP neural network.

Model	Mean absolute error	Correlation coefficient
Improved double hidden layer	0.11	0.69
Single hidden layer	0.17	0.41

TABLE 6. Ratio of new energy trans-regional absorbed transmission power to L region accepted power.

Month	January	February	March	April	May	June	July	August	September	October	November	December
Ratio	0.85	0.88	0.87	0.90	0.92	0.90	0.95	0.89	0.87	0.89	0.95	0.96

Table 6 describes the ratio of trans-regional absorption and transmission power of new energy to the accepted power in L region. The ratio of trans-regional absorbed transmission power of new energy to accepted power in L region reflects that new energy power can be accepted and utilized by power network in L region to some extent. The size of this ratio is influenced by many factors. If the ratio is high, it shows that the new energy power can be fully absorbed and utilized by the local power network, and the surplus part of new energy power generation is less; If the ratio is low, it shows that the new energy power cannot be accepted and utilized by the local power network to some extent, and there is a certain surplus of new energy power.

According to the data in Table 6, after the application of this method, the ratio of the trans-regional consumption and transmission power of new energy to the accepted power in L area is higher than 0.85, and the maximum value can reach 0.96, which shows that the new energy in this area has been fully utilized in the trans-regional transmission process. The consumption and transmission power prediction of this method can effectively guide the rational transmission of new energy in this area, ensure the high proportion of new energy consumption, and avoid a large number of abandoned wind and electricity phenomena.

Firstly, in terms of effectiveness, this method predicts the cross regional absorption and transmission power of new energy through a double hidden layer BP neural network, and combines the fluctuation of new energy output, capacity confidence, peak shaving characteristic parameters, and relevant parameters provided by numerical weather forecasting. This comprehensive multi factor approach can comprehensively consider various factors that affect the absorption capacity of new energy, thereby improving the accuracy of predictions. Experimental results have shown that this method can accurately predict the cross regional absorption and transmission power of new energy, and the ratio of predicted power to received power is greater than 0.85, which fully demonstrates the effectiveness of this method. Secondly, in terms of robustness, this method adopts the SSA to optimize the weights and thresholds of the double hidden layer BP neural network, avoiding the situation of over training falling into local optima. This optimization strategy helps to improve the generalization ability of the model, enabling it to maintain good predictive performance when facing different datasets and scenarios. In addition, this method also normalizes the sample data, further improving the robustness and adaptability of the model.

In summary, the method proposed in this article has good power prediction performance because it fully considers the volatility of new energy output in the prediction model. By selecting appropriate characteristic parameters such as fluctuations in new energy output, capacity confidence, and peak shaving characteristic parameters, it can more accurately reflect the actual operation of new energy power generation. The double hidden layer BP neural network can better learn and simulate the complex patterns and trends of new energy output power, and has strong nonlinear mapping and generalization abilities. This network structure can better handle the volatility of new energy output, improve the accuracy and stability of predictions. This method optimizes the weights and thresholds of the double hidden layer BP neural network using the SSA, avoiding the problem of over training local optima. The application of optimization algorithms can improve the training efficiency and generalization ability of neural networks, making the prediction results more reliable.

4. Conclusion

The fluctuation in new energy production, low confidence in capacity, significant regional differences, and low contribution rate to peak shaving have seriously affected the level of new energy consumption. Based on the dual hidden layer BP neural network and sparrow search algorithm, taking into account factors such as new energy volatility and capacity confidence, the predictive performance is improved through standardized processing, which has the advantage of high-precision prediction of power fluctuations in cross regional absorption and transportation of new energy. However, its computational complexity is high, it depends on data quality and quantity, and requires adjustment of optimization parameters, while lacking dynamic adaptability to new environmental changes. Future research work can focus on the following aspects: Firstly, to address the computational complexity of the model, more efficient optimization algorithms and neural network structures can be explored to reduce training time and computational resource consumption, and improve real-time prediction ability. Secondly, regarding the issue of dependence on data quality and quantity, future research can focus on data augmentation and feature extraction techniques. By synthesizing more high-quality sample data or extracting more representative features, the generalization ability and robustness of the model can be enhanced.

References

[1] M.T. Ahammed and I. Khan, Ensuring power quality and demand-side management through IoT-based smart meters in a developing country. *Energy* **250** (2022) 123747.1–123747.19.

[2] M. Gholami, O. Shahryari, N. Rezaei and H. Bevrani, Optimum storage sizing in a hybrid wind-battery energy system considering power fluctuation characteristics. *J. Energy Storage* **52** (2022) 104634.1–104634.10.

[3] B. Carrera, M.K. Sim and J.Y. Jung, PvHybNet: a hybrid framework for predicting photovoltaic power generation using both weather forecast and observation data. *IET Renew. Power Gener.* **143** (2020) 2192–2201.

[4] G. Memarzadeh and F. Keynia, Short-term electricity load and price forecasting by a new optimal LSTM-NN based prediction algorithm. *Electr. Power Syst. Res.* **192** (2021) 106995.1– 106995.14.

[5] A. Onno, N. Rodkey, A. Asgharzadeh, S. Manzoor, Z.J. Yu, F. Toor and Z.C. Holman, Predicted power output of silicon-based bifacial tandem photovoltaic systems. *Joule* **4** (2020) 580–596.

[6] Y. Wang, S. Luo and Z. Wang, Photovoltaic power prediction combined with popular learning and improved BP neural network. *Comput. Simul.* **39** (2022) 153–157.

[7] J. Arevalo-Soler, E. Sanchez-Sanchez, E. Prieto-Araujo and O. Gomis-Bellmunt, Impact analysis of energy-based control structures for grid-forming and grid-following MMC on power system dynamics based on eigenproperties indices. *Int. J. Electr. Power Energy Syst.* **143** (2022) 108369.1–108369.15.

[8] T. Nasmark and J. Andersson, Proton stopping power prediction based on dual-energy CT-generated virtual monoenergetic images. *Med. Phys.* **48** (2021) 5232–5243.

[9] G. Raina, S. Sinha, G. Saini, S. Sharma, P. Malik and N.S. Thakur, Assessment of photovoltaic power generation using fin augmented passive cooling technique for different climates. *Sustain. Energy Technol. Assess.* **52** (2022) 102095.1–102095.17.

[10] S. Ma, Cross-regional analysis of new energy consumption capacity. *J. Beijing Inst. Technol.* **29** (2020) 38–44.

[11] A. Saeed, C. Li, Z. Gan, Y. Xie and F. Liu, A simple approach for short-term wind speed interval prediction based on independently recurrent neural networks and error probability distribution. *Energy* **238** (2022) 122012.1–122012.14.

[12] M. Pierro, M. De Felice, E. Maggioni, D. Moser, A. Perotto, F. Spada and C. Cornaro, Data-driven upscaling methods for regional photovoltaic power estimation and forecast using satellite and numerical weather prediction data. *Solar Energy* **158** (2017) 1026–1038.

[13] A. Gulagi, M. Ram and C. Breyer, Role of the transmission grid and solar wind complementarity in mitigating the monsoon effect in a fully sustainable electricity system for India. *IET Renew. Power Gener.* **14** (2020) 254–262.

[14] F. Rodríguez, A. Galarza, J.C. Vasquez and J.M. Guerrero, Using deep learning and meteorological parameters to forecast the photovoltaic generators intra-hour output power interval for smart grid control. *Energy* **239** (2022) 122116.1–122116.13.

[15] V. Repecho, N. Masclans and D. Biel, A comparative study of terminal and conventional sliding-mode startup peak current controls for a synchronous buck converter. *IEEE J. Emerg. Sel. Topics Power Electron.* **9** (2021) 197–205.

[16] M. Tajdinian, M. Allahbakhshi, M. Mohammadpourfard, B. Mohammadi, Y. Weng and Z. Dong, Probabilistic framework for transient stability contingency ranking of power grids with active distribution networks: application in post disturbance security assessment. *IET Gener. Transm. Distrib.* **14** (2020) 719–727.

[17] W.M. Ebrahimi, Retraining deep neural network with unlabeled data collected in embedded devices. *J. Electron.* **20** (2022) 55–69.

[18] R. Thenmozhi, A.W. Nasir, V.K. Sonthi, T. Avudaiappan, S. Kadry, K. Pin and Y. Nam, An improved sparrow search algorithm for node localization in WSN. *CMC-Comput. Mater. Continua* **71** (2022) 2037–2051.

[19] H. Peng, Y. Wen, Q. Wang, S. Wang and L. Wu, Crack detection in eggs with multi-level wavelet transform and BP neural network. *Trans. Chin. Soc. Agric. Mach.* **40** (2009) 170–174.

[20] Y. Qiu and L. Zhao, Impact resistance prediction of fuselage coatings based on improved neural network. *Ordnance Mater. Sci. Eng.* **45** (2022) 148–153.

Please help to maintain this journal in open access!

This journal is currently published in open access under the Subscribe to Open model (S2O). We are thankful to our subscribers and supporters for making it possible to publish this journal in open access in the current year, free of charge for authors and readers.

Check with your library that it subscribes to the journal, or consider making a personal donation to the S2O programme by contacting subscribers@edpsciences.org.

More information, including a list of supporters and financial transparency reports, is available at https://edpsciences.org/en/subscribe-to-open-s2o.